

Visakhapatnam Chapter

*Proceedings of Indian Geotechnical Conference 2020
December 17-19, 2020, Andhra University, Visakhapatnam*

Active Earth Pressure Distribution against Braced Wall Considering Arching Effects

Kingshuk Dan¹ and Ramendu Bikash sahu²

¹ Coochbehar Govt Engineering College, Coochbehar 736170, West Bengal, INDIA
kingshuk.dan@gmail.com

² Jadavpur University, Jadavpur, Kolkata 700032, West Bengal, INDIA

Abstract. Estimation of active earth pressure against the rigid wall depends on the mode of wall movement. The pressure distribution is non linear owing to arching effects. Here new formulations of calculating active earth pressure above and below cut level are proposed considering arching effects against braced wall. Horizontal translation as well as rotation about the top of wall is taken into account for above excavation whereas below cut level the wall is tilting around its lower edge. Expressions for earth pressure coefficient, earth pressure distribution and total earth pressure force are provided considering soil parameters like soil friction angle ' ϕ ', wall friction angle ' δ ' and cohesion ' c ' etc. For validation of the proposed formulation, the predicted values are compared with existing case studies. Comparisons between measured and predicted values establish that proposed method satisfactorily predict earth pressure exerted on wall for both cohesive and cohesionless soil.

Keywords: Arching effect, Stress distribution, Wall movement, Case study

1 Introduction

Adequate prediction of active earth pressure is major design consideration of retaining structure. Distribution of earth pressure is practically non-linear depending on mode of wall movement, friction mobilization between soil and wall, wall rigidity, spacing of lateral support etc. Thus consideration of arching during estimation of earth pressure against retaining wall is necessary. Various researchers proposed formulations of earth pressure distribution behind wall considering translational or rotational movement of wall [1], [2], [3], [4]. But very limited works have been done for braced excavation. In present study a formulation for calculating active earth pressure on a braced wall is proposed considering arching effects where effect of cohesion, angle of wall friction, angle of shearing resistance are taken into account. In order to validate, results obtained from proposed method are compared with the existing field values of three case studies reported by Som et al. (1991) [5], Goh et al. (2005) [6], Liu et al. (2005) [7].

In the present study, translation along with rotation of wall about top for above cut level is assumed while in below cut level it is taken that wall rotates about its base. Considering all these types of yielding a planar slip surface making an angle of $(45^\circ + \phi/2)$ with horizontal is assumed. Movement of ground surfaced is assumed to be

spandrel type which is because considerable amount of wall deflection occurs before installing strut. Below cut level maximum vertical ground movement is assumed to occur at some distance from wall (Fig. 1).

2 Theoretical Study

Above cut level an arc of a circle of convex type is taken into consideration. Here slip plane makes an angle of $(45^\circ + \phi/2)$ with the minor principal stress at the right edge of the element. Major Principal Plane makes an angle of ' ψ ' with horizontal, where, ' ψ ' varies from 0 at right edge to ' θ ' at left edge (Fig. 2).

From force equilibrium, at any point on arch it can be written as

$$\sigma_h = \sigma_3 \cos^2 \psi + \sigma_1 \sin^2 \psi \tag{1}$$

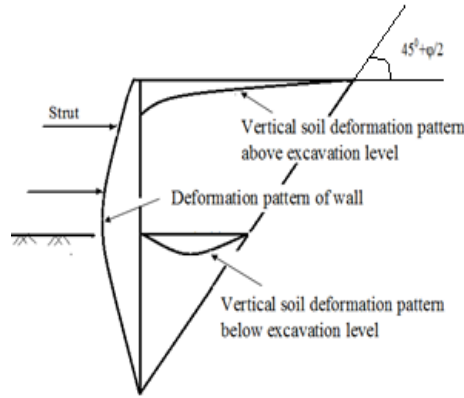


Fig. 1. Slip surface and soil deformation pattern

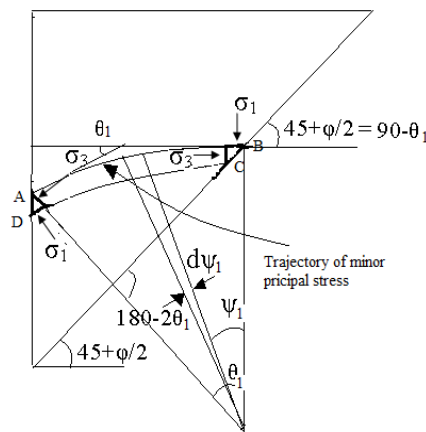


Fig. 2. Stress distribution on differential soil element

For calculation of ‘ θ ’, Mohr circle for stresses of soil element at edge of wall is considered (Fig. 3).

$$\tau_w = C_a + \sigma_{h,wall} \tan \delta = (\sigma_{h,wall} - \sigma_3) \tan(90 - \theta) \quad (2)$$

Here ‘ C_a ’ is adhesion of soil with wall which can be obtained from expression. Here, ‘ a ’ is adhesion factor.

$$C_a = a \times c \quad (3)$$

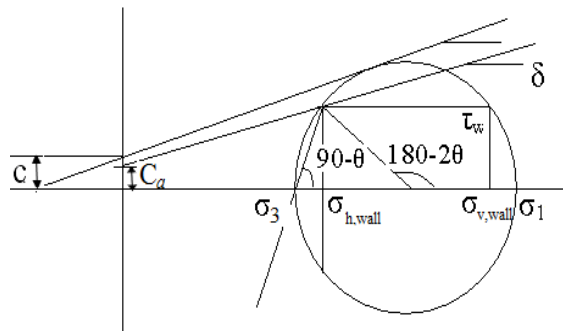


Fig. 3. Mohr circle for stresses at wall

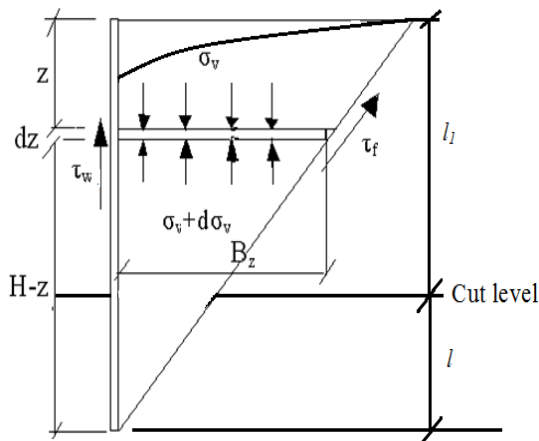


Fig. 4. Free body diagram of differential soil element

Eq. (2) can be further reduced as

$$\tan(90^\circ - \theta) = \frac{(\sigma_{h,wall} / \sigma_3) \tan \delta + (C_a / \sigma_3)}{(\sigma_{h,wall} / \sigma_3) - 1} \quad (4)$$

The expression of ‘ θ ’ can be written as

$$\theta = \tan^{-1} \left[\frac{(N-1) \pm \sqrt{(N-1)^2 - 4(m + \tan \delta)(m + N \tan \delta)}}{2(m + N \tan \delta)} \right] \quad (5)$$

Where, $m = \frac{C_a}{\sigma_3}$ and ‘ N ’ is the ratio of major and minor principal stress

Average vertical stress over a differential element ‘ABCD’ at a depth ‘ Z ’ below ground surface as shown in Fig. 2 will be

$$\bar{\sigma}_v = \frac{F}{B_z} = \frac{1}{B_z} \int_0^\theta dF = \frac{1}{B_z} \int_0^\theta \sigma_v dA = \frac{1}{R \sin \theta} \int_0^\theta \sigma_1 \left(\cos^2 \psi + \frac{1}{N} \sin^2 \psi \right) R d\psi \cos \psi \quad (6)$$

Integrating equation 6 yields

$$\bar{\sigma}_v = \sigma_1 \left[\frac{3N+1}{4N} + \frac{N-1}{12N} (3 - 4 \sin^2 \theta) \right] \quad (7)$$

Active earth pressure co-efficient at the wall will be

$$K_{wall} = \frac{\sigma_{h,wall}}{\bar{\sigma}_v} = \frac{(1/N) \cos^2 \theta + \sin^2 \theta}{\left(\frac{3N+1}{4N} \right) + \frac{N-1}{12N} (3 - 4 \sin^2 \theta)} \quad (8)$$

From the stresses acting on differential element of ‘ dZ ’ behind braced wall (Fig. 4) force equilibrium is established in vertical direction.

$$d\bar{\sigma}_v B_z = dZ (\gamma B_z - (C_a + \bar{\sigma}_v K_{wall} \tan \delta)) \quad (9)$$

Solving equation 9 the expression of average vertical stress will be

$$\begin{aligned} \bar{\sigma}_v K_{wall} \tan \delta (\tan \alpha \tan \delta K_{wall} - 1) &= (aC_0 + aC_1 H) (\tan \alpha \tan \delta K_{wall} - 1) \left[\left(1 - \frac{Z}{H}\right)^{\tan \alpha \tan \delta K_{wall}} - 1 \right] \\ &+ (aC_1 \tan \alpha - \gamma) \tan \delta K_{wall} \left[H \left(1 - \frac{Z}{H}\right)^{\tan \alpha \tan \delta K_{wall}} - (H - Z) \right] \end{aligned} \quad (10)$$

Where, $c = C_0 + C_1 Z$, where, C_0 is initial cohesion at ground surface and C_1 is the rate of increase of cohesion with depth.

The active lateral stress at any depth 'Z' acting on the wall

$$\sigma_{h,wall} = \frac{(aC_0 + aC_1 H)}{\tan \delta} \left[\left(1 - \frac{Z}{H}\right)^{\tan \alpha \tan \delta K_{wall}} - 1 \right] + \frac{(aC_1 \tan \alpha - \gamma) K_{wall}}{(\tan \alpha \tan \delta K_{wall} - 1)} \left[H \left(1 - \frac{Z}{H}\right)^{\tan \alpha \tan \delta K_{wall}} - (H - Z) \right] \quad (11)$$

Similarly analysis have been done for below cut level and lateral stress distribution

$$\begin{aligned} \sigma_{h,wall}' &= \frac{(aC_0' + aC_1 l)}{\tan \delta'} \left[\left(1 - \frac{Z'}{l}\right)^{\tan \alpha \tan \delta' K_{wall}'} - 1 \right] + \frac{(aC_1 \tan \alpha - \gamma) K_{wall}'}{(\tan \alpha \tan \delta' K_{wall}' - 1)} \left[l \left(1 - \frac{Z'}{l}\right)^{\tan \alpha \tan \delta' K_{wall}'} - (l - Z') \right] \\ &+ \left[(X \times K_{wall}') \left(1 - \frac{Z'}{l}\right)^{\tan \alpha \tan \delta' K_{wall}'} \right] \end{aligned} \quad (12)$$

Where,

$$X = \frac{(aC_0 + aC_1 H)}{\tan \delta} \left[\left(\frac{l}{H}\right)^{\tan \alpha \tan \delta K_{wall}} - 1 \right] + \frac{(aC_1 \tan \alpha - \gamma) K_{wall}}{(\tan \alpha \tan \delta K_{wall} - 1)} \left[H \left(\frac{l}{H}\right)^{\tan \alpha \tan \delta K_{wall}} - l \right] \quad (13)$$

Total lateral active force on wall obtained as

$$P_h = \int_0^{l_1} \sigma_{h,wall} dZ + \int_{l_1}^H \sigma_{h,wall}' dZ' \quad (14)$$

Solving equation 14 we can get

$$P_h = \frac{-(aC_0 + aC_1 H)H \tan \alpha K}{\tan \alpha \tan \delta K + 1} + \frac{(aC_1 \tan \alpha - \gamma)KH^2}{\tan \alpha \tan \delta K - 1} \left[\frac{1}{\tan \alpha \tan \delta K + 1} - \frac{1}{2} \right]$$

(15)

3 Case Study

3.1 Kolkata Metro Construction [5]

Braced excavation varied in depth from 9-14 m was made with 600 mm RCC diaphragm wall propped by steel struts. The soil stratification at the site consists of desiccated brownish silty clay (upto 14 m) with cohesion value of 25 kN/ m² and soil unit weight of 18 kN/ m³ followed by stiff clay (c = 60 kN/ m²). Predicted values are plotted with measured active earth pressure (Fig. 5).

3.2 An Idealized deep excavation [6]

An idealized 18 m deep braced excavation was analyzed by continuous beam method where idealized soil profile of sand layer with uniform friction angle of $\phi = 30^0$ and unit weight of 19 kN/ m³ were assumed. Five stages of excavation were considered where final stage was done at a depth of 60 m with wall embedment depth of 6 m. The computed earth pressure at final stage of excavation by the use of continuous beam method is compared with the results obtained from proposed method (Fig. 6).

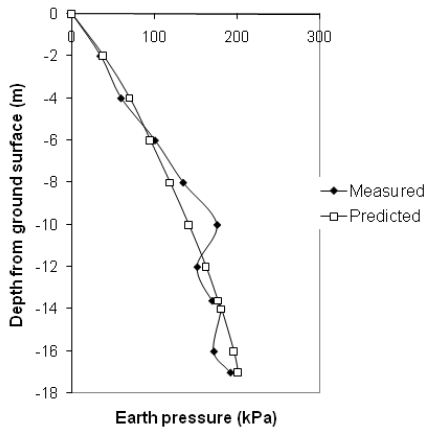


Fig. 5. Earth pressure distribution at Kolkata Metro Construction

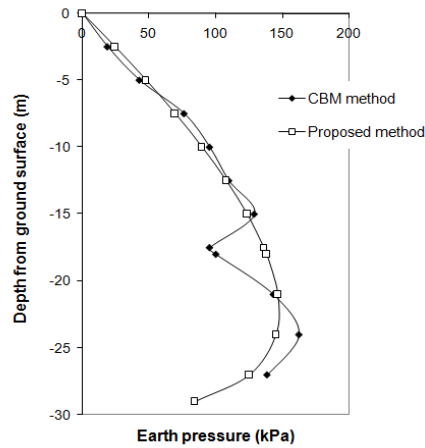


Fig.6. Active earth pressure distribution for an idealized 18 m deep excavation

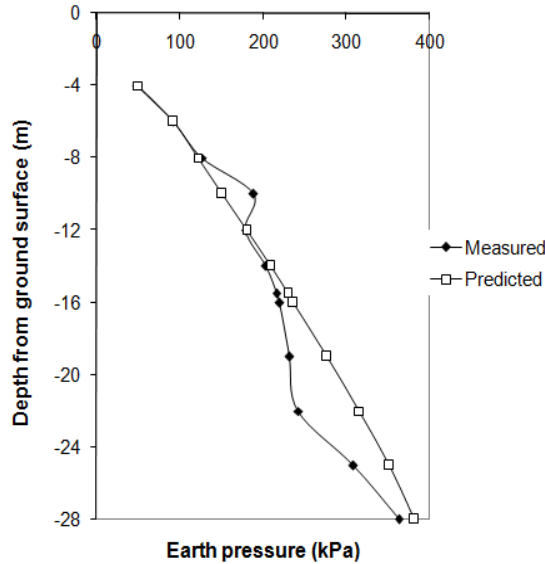


Fig. 7. Active earth pressure distribution at final stage of Shanghai Metro Station

3.3 Excavation in Shanghai soft clay [7]

The excavation was supported by a 0.6 m thick, 28 m deep concrete diaphragm wall with final excavation depth was 15.5 m. Five levels of bracings were installed before reaching final stage of excavation. The uppermost clay layer appeared to be desiccated and it has higher shear strength than underlain marine deposits of soft silty and medium clay. Here active earth pressure along wall is predicted considering measured cohesion value simulating clayey nature of soil. The result is shown in Fig. 7.

4 Conclusions

In present study a new method is proposed for estimation of earth pressure distribution against diaphragm wall, both translating and rotating, considering arching effects assuming shape of arches as arc of circles for above and below excavation. This proposed formulation can be used for both cohesive and cohesionless soil as the expressions consist of cohesion and angle of internal friction. From the comparison with the published results of previous investigators and measured values, it is observed that formulation produce satisfactory prediction of earth pressure distributions in any kind of soil.

References

1. Handy, R.L.: The arch in soil arching. *Journal of Geotechnical Engineering, ASCE* 111(3), 302-318 (1985).
2. Goel, S., Patra, N. R.: Effect of arching on active earth pressure for rigid retaining walls considering translation mode. *International Journal of Geomechanics, ASCE* 8(2), 123-133 (2008).
3. Paik, K.H. and Salgado, R.: Estimation of active earth pressure against rigid retaining walls considering arching effects. *Geotechnique* 53 (7), 643-653 (2003).
4. Rao, P., Chen, Q., Zhou, Y., Nimbalkar, S. and Chiaro, G.: Determination of active earth pressure on rigid retaining wall considering arching effect in cohesive backfill soil, *International Journal of Geomechanics, ASCE* 16 (3), 1-9 (2016).
5. Som, N.N.: Performance study of braced cuts for calcutta metro construction. *Proceedings of 9th Asian Regional Conference on SMFE*, pp 387-394. Bangkok, Thailand (1991).
6. Goh, S.H., Semple, R. M., Tamaro, G.J.: Comparison of finite element and continuous beam methods for excavation support design. *Structures Congress 2005: Metropolis and Beyond*, ASCE, New York, United States (2005).
7. Liu, G.B., Ng, C.W.W. and Wang, Z.W.: Observed performance of a deep multistrutted excavation in shanghai soft clays. *Journal of Geotechnical and Geoenvironmental Engineering, ASCE* 131(8), 1004-1013 (2005).